

Climate Characteristics of Record-heavy Rain and Record-low Sunshine

Durations in Japan in July 2020

16 September 2020

Tokyo Climate Center, Japan Meteorological Agency

<https://ds.data.jma.go.jp/tcc/tcc>

Summary

- In July 2020, western to northeastern Japan experienced record-heavy rain and record-low sunshine durations.
- The month was characterized by a remarkable series of heavy rainfall events from western to eastern Japan from 3rd to 31st July. In some areas, monthly precipitation totals exceeded 2 to 2.4 times the climatological normal, making the period the wettest since 1946 when records began.
- These phenomena are attributed to a continued tendency for large amounts of water vapor to concentrate around western and eastern Japan from two major flows – one from the west along the Meiyu-Baiu front, which stagnated along mainland Japan due to delayed northward migration of the subtropical jet stream, and the other from the south along the periphery of the North Pacific Subtropical High, which extended southwestward of its climatological extent.
- A persistent upper-level trough over the Yellow Sea also caused an intensification of Meiyu-Baiu front activity with enhanced vertical upward flow over western and eastern Japan, resulting in prolonged heavy rain.
- The delayed northward migration of the subtropical jet stream and the southwestward expansion of the North Pacific Subtropical High may be attributable to higher-than-normal sea surface temperatures (SSTs) in the Indian Ocean and related inactivity of the Asian summer monsoon.

1. Climate conditions

In July 2020, with the stagnation of the active Meiyu-Baiu front¹ over Japan, rainy conditions were prominent over the Kyushu region and a wide area from western to eastern parts of the country. In particular, prefectures in the Kyushu region and elsewhere experienced unprecedented rainfall during the first 10 days of the month, causing widespread disruption. The last 10 days of the month saw heavy rain causing damage in the Tohoku region of Japan,

¹ A seasonal rain belt that appears at the border between the warm and moist tropical air mass over the Pacific and the relatively cool and dry air mass over the Asian continent and subpolar seas in early summer, characterized by a significant gradient of equivalent potential temperature.

including an overflow of the Mogami River in Yamagata Prefecture.

In the Kyushu region and other locations (including the prefectures of Gifu, Nagano and Yamagata), numerous weather stations reported record precipitation amounts. In particular, maximum precipitation values for 1-, 3-, 6-, 12-, 24-, 48- and 72-hour periods were unprecedented during the period from 3rd to 31st July, 2020 (Figure 1-1). In the Tohoku region, on the Pacific side of eastern/western Japan and on the Sea of Japan side of western Japan, monthly precipitation totals exceeded 2 to 2.4 times the monthly climatological normal, making the period the wettest since 1946 when records began (Table 1-1 and Figure 1-2, middle).

The Baiu season in the Amami region did not end until around 20th July, making it the latest on record. In other areas, the Baiu rainy season ended around 10 days later than the climatological normal. In the Kanto-Koshin region the season did not end until around 1st August, which was far later than the climatological normal, with many observation stations recording rainfall every day.

Monthly sunshine durations were extremely short. In the Tohoku region, on the Pacific side of eastern/western Japan and on the Sea of Japan side of eastern/western Japan, durations were around half the climatological normal – the lowest for each region since 1946 when records began (Table 1-2, Figure 1-2, bottom).

In nearby countries, the active Meiyu-Baiu front over Central China brought unprecedented rainfall over the Yangtze River basin from June to July 2020 (Figure 1-3). In Nanchang in Jiangxi Province, the monthly precipitation of 693 mm was the highest since 1982 (far exceeding the previous record of 457mm (1998)). This was also associated with the prolonged activity of the front.

2. Characteristics of atmospheric circulation associated with the heavy rain events of July 2020 (Figure 2-1)

During the prolonged period of heavy rainfall, the Meiyu-Baiu front was intensified and remained near-stationary over or close to the area from western to eastern Japan. This was primarily because 1) a persistent upper-level trough over the Yellow Sea enhanced ascending air flow downstream over Japan, and 2) the subtropical jet stream (STJ), which in a normal summer gradually migrates northward and reaches latitudes north of 40°N by mid-July, continued to flow over the area from western to eastern Japan and locked the Meiyu-Baiu front in a narrow latitude band.

The persistent trough was in turn sustained by a semi-circumglobal quasi-stationary Rossby wave train propagating eastward along the STJ over Eurasia (known as the Silk Road teleconnection) (Enomoto et al, 2003; Kosaka et al, 2009). This wave pattern may have been partly attributable to influences from the mountainous topography of the Tibetan Plateau on the STJ. The southward displacement of the STJ was attributable to the weaker-than-normal

Tibetan High with its eclipsed northward extension, likely in relation to suppressed convective activity over the Asian summer monsoon region from India to the seas east of the Philippines and elsewhere.

Meanwhile in the lower troposphere, the North Pacific Subtropical High (NPSH) extended southwestward of its climatological extent. This anomalous anticyclonic circulation to the south of Japan enhanced summer-monsoon southwesterlies around the country. In association, vast moist air inflows conveying masses of water vapor to the Meiyu-Baiu front continued to converge over areas from western to eastern Japan (Figure 2-2), where there was a major moisture inflow from the west along the front and another from the south along the periphery of the NPSH.

SSTs were higher than normal over the area from Indonesia to the tropical Indian Ocean, which led to enhanced convective activity in the area and particularly over the western Indian Ocean. This induced lower-troposphere convergence anomalies over areas from the Indian Ocean to Indonesia and divergence anomalies from the South China Sea to the western tropical Pacific. These large-scale tropical circulation anomalies gave rise to descending air flow and suppressed convective activity over the South China Sea and the western tropical Pacific. This suppression likely contributed to the southwestward extension of the NPSH.

The above-normal SSTs observed in the Indian Ocean may be attributable to a positive phase of the Indian Ocean Dipole (IOD) (Saji, 1999) that continued from summer to autumn 2019. During this IOD episode, a significantly warm water mass developed in the central South Indian Ocean and started to propagate westward in early 2020, contributing to sustained higher SSTs in the western part. From June 2020 onwards, the weaker-than-normal southwest monsoon can be seen as another possible factor behind the warm SSTs in the Indian Ocean.

On a long time scale, atmospheric water vapor content has been rising at a rate consistent with thermodynamic expectations in association with the long-term warming trend; that is, around 7% per 1°C of warming (Figure 2-3). A preliminary simulation using a mesoscale numerical model indicates that the total precipitation from the heavy rain event of July 2020 was increased by this higher atmospheric content of water vapor; in other words, this level of precipitation would not have occurred without global warming. However, event attribution research and other forms of closer quantitative analysis to clarify the degree of influence from long-term climate change is needed.

3. Line-shaped precipitation systems – a case in Kyushu region from 3 to 8 July 2020 –

The heavy rainfall observed over Kumamoto Prefecture from 3 to 4 July was brought about by line-shaped precipitation systems associated with large amounts of lower-level water vapor flowing into the region and a series of cumulus clouds that formed on the windward side (Figure 3). Heavy rainfall over the northern Kyushu region on 6 July was also caused by formations of multiple line-shaped precipitation systems.

References

- Enomoto, T., B. J. Hoskins and Y. Matsuda, 2003: The formation mechanism of the Bonin high in August. *Quart. J. Roy. Meteor. Soc.*, **129**, 157–178.
- Kobayashi, S., Y. Ota, Y. Harada, A. Ebita, M. Moriya, H. Onoda, K. Onogi, H. Kamahori, C. Kobayashi, H. Endo, K. Miyaoka and K. Takahashi, 2015: The JRA-55 Reanalysis: General specifications and basic characteristics. *J. Meteor. Soc. Japan*, **93**, 5–48.
- Kosaka, Y., H. Nakamura, M. Watanabe, M. Kimoto, 2009: Analysis on the Dynamics of a Wave-like Teleconnection Pattern along the Summertime Asian Jet Based on a Reanalysis Dataset and Climate Model Simulations. *J. Meteor. Soc. Japan*, **87**, 561-580.
- Saji, N. H. et al., 1999: A dipole mode in the tropical Indian Ocean. *Nature* **401** (6751), 360–3. doi:10.1038/43854.

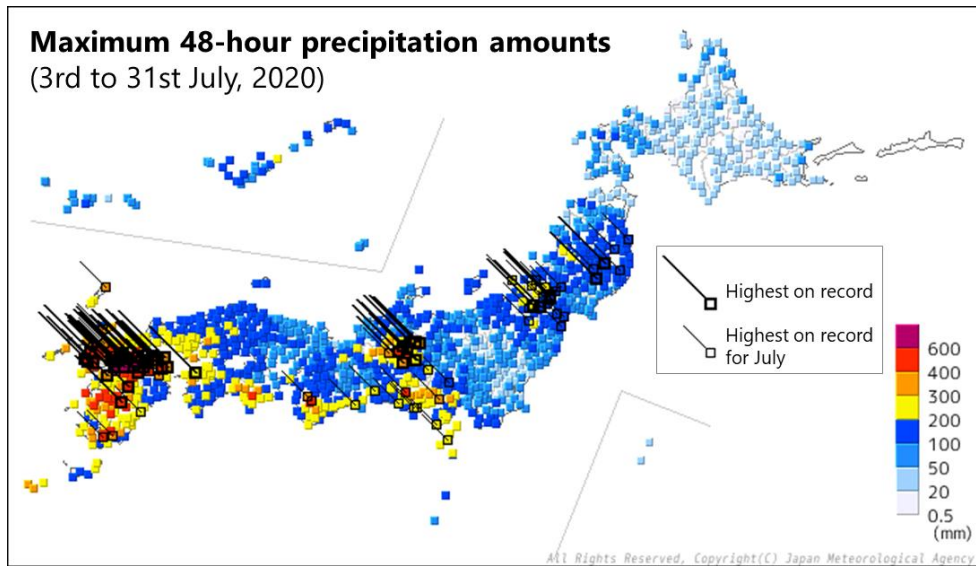


Figure 1-1. Maximum 48-hour precipitation amounts (3rd to 31st July, 2020)

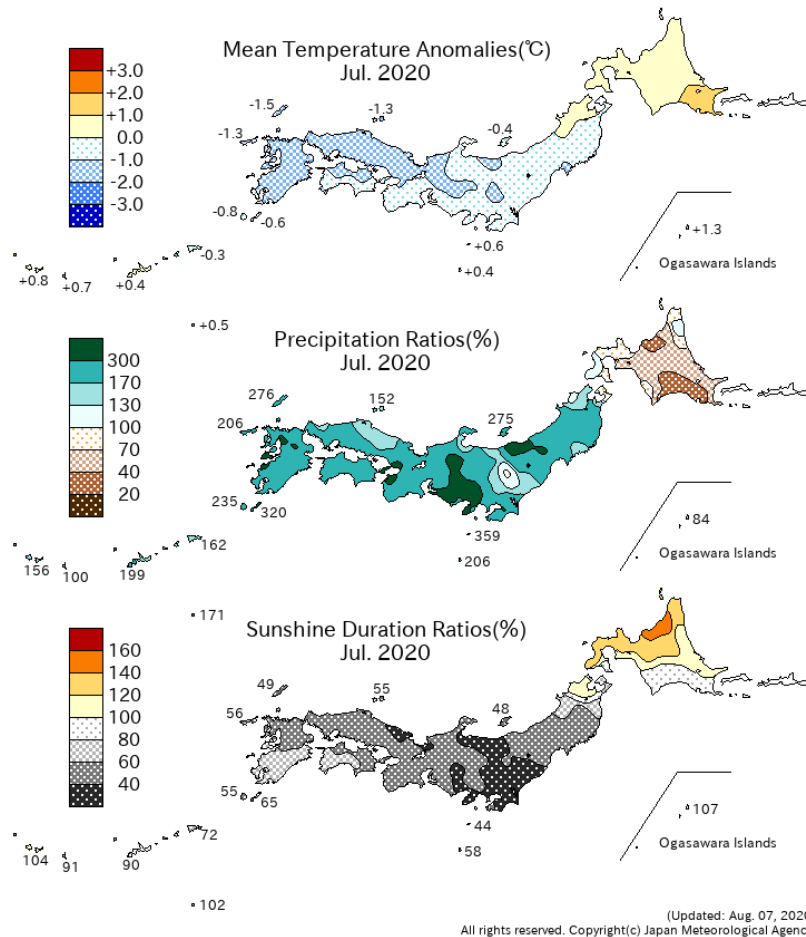


Figure 1-2. Mean temperature anomalies, precipitation ratios and sunshine duration ratios for July 2020.

The base line period for the normal is 1981 –2010

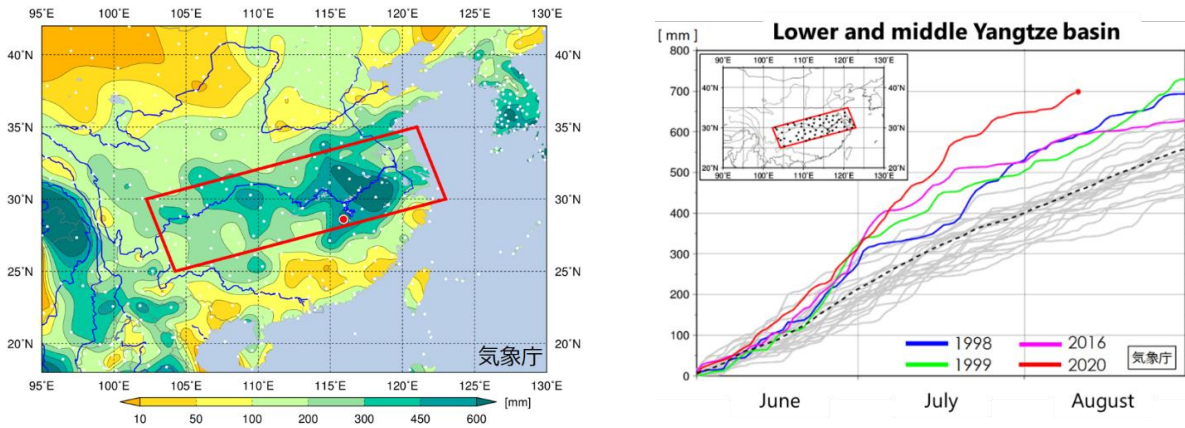


Figure 1-3. Heavy rain along the Yangtze river basin from June to August 2020

[Left] Precipitation totals for July 2020

This map was created using weather observation reports from National Meteorological Services of the relevant countries. White dots represent weather observation stations, and the red dot indicates the location of Nanchang in China’s Jiangxi Province. The red box shows the range of points used for calculation of cumulative precipitation (right).

[Right] Cumulative rainfall over the lower and middle Yangtze Basin

Unit: mm. The lines show cumulative rainfall averaged over 60 observation stations in the lower and middle Yangtze basin (red frame) based on weather observation reports from the China Meteorological Agency. Red line: cumulative time-series representation of precipitation for boreal summer 2020; purple, green, blue, other: the same for the summers of 2016, 1999, 1998 and others after 1997; dashed: 23-year averages (1997 – 2019).

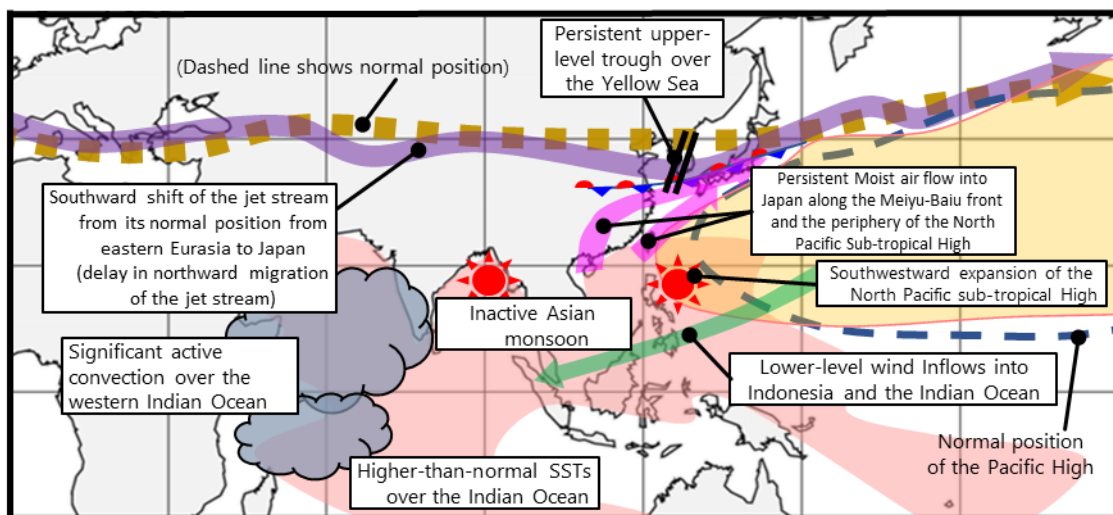
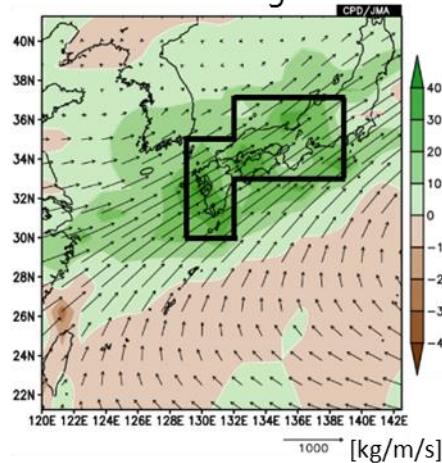


Figure 2-1. Atmospheric circulation conditions associated with the climate extremes observed in July 2020

(a) Vertically integrated water vapor flux and its convergence



(b) Water vapor amounts concentrated in western and eastern Japan

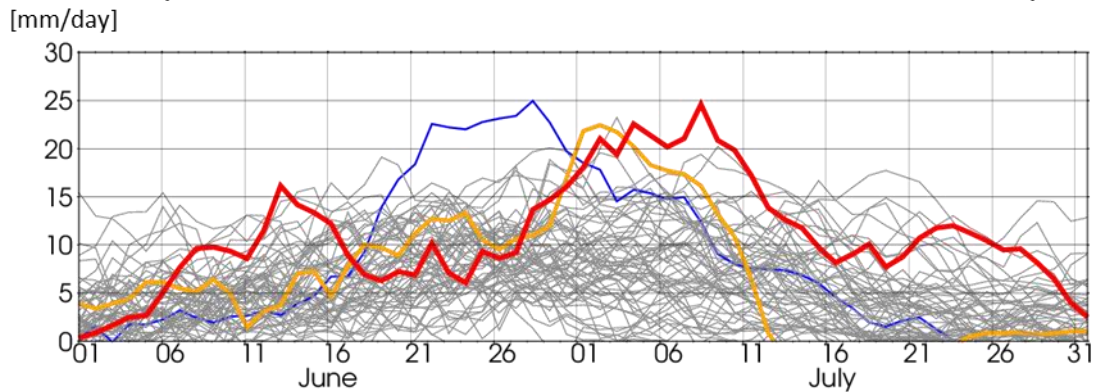


Figure 2-2. (a) Vertically integrated horizontal water vapor flux (arrows) and its convergence (shade) averaged over the period from 3rd to 13th July 2020 and (b) time-series representation of vertically integrated water vapor flux convergence (the 11-day running mean) in the area surrounded by the black lines in (a) from June to July after 1958

(a) Unit: kg/m/second for arrows and mm/day for shade.

(b) Unit: mm/day. Data for the period from 1958 to 2020 are overlaid into one calendar year. The red, blue, orange and gray indicate values for 2020, 1985 (a heavy rain event related to Meiyu-Baiu front and a typhoon), 2018 (The heavy rain event of July 2018) and others after 1958, respectively.

(a) and (b) are generated from JRA-55 data (Kobayashi, 2015), and vertical integration here represents integration from the surface to 300hPa.

Specific humidity ratio at 850hPa for July in Japan

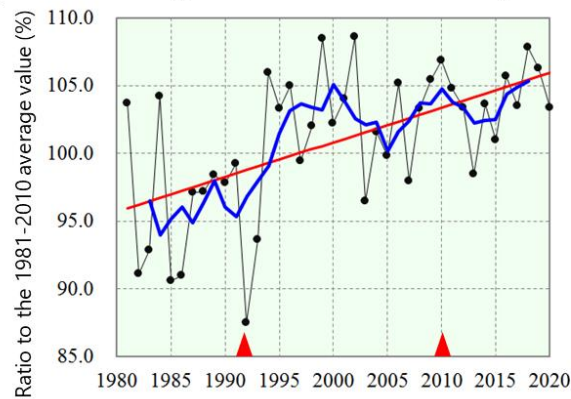


Figure 2-3. Specific humidity ratio at 850 hPa for July from 1981 to 2020 in Japan

The data are presented as ratios against the baseline (the 1981 – 2010 average).

Note: The term specific humidity refers to the mass of water vapor in a unit mass of moist air (g/kg). The data used in this analysis were based on radiosonde observations (balloon-borne instrument platforms with a radio-transmitting device) at 13 upper-air observation stations in Japan. The dots show the averages of the data for the 13 stations. The thick blue line indicates the five-year running mean, and the straight red line indicates the long-term linear trend (statistically significant at a confidence level of 99%). Data from the period marked by the red triangles may include biases due to instrument changes.

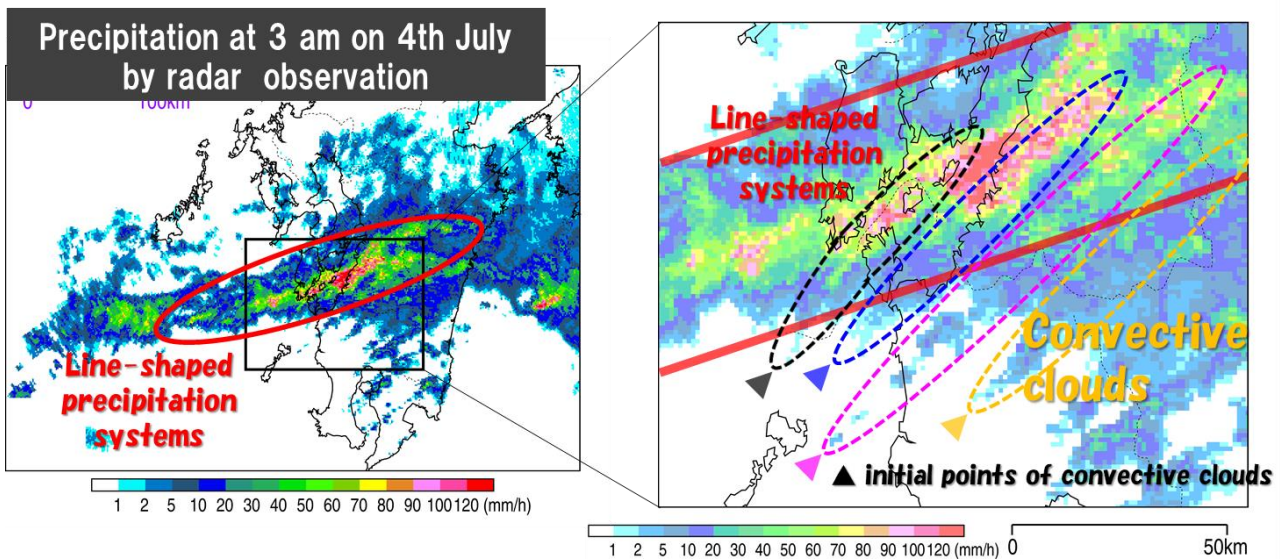


Figure 3. Structure of line-shaped precipitation systems (3 a.m. on 4th July, 2020) based on JMA's gridded radar precipitation analysis products

Multiple convective clouds (dotted circles in the figure on the right) extending from SW to NE form a linear precipitation system (red circle in the figure on the left). The triangles in the figure on the right represent initial points of convective genesis.

Table 1-1. Years of wettest Julys in Japan and related precipitation ratios against the climatological normal

	Tohoku region	The Sea of Japan side of eastern Japan	The Pacific side of eastern Japan	The Sea of Japan side of western Japan	The Pacific side of western Japan
Rank 1	2020 (201%)	1964 (229%)	2020 (245%)	2020 (222%)	2020 (240%)
Rank 2	2013 (182%)	2006 (228%)	1974 (187%)	1957 (212%)	1993 (236%)
Rank3	2002 (169%)	1995 (211%)	1993 (181%)	1980 (195%)	1951 (205%)

Statistics began in 1946

Table 1-2. Years of shortest sunshine durations in Japan for July and related ratios against the climatological normal

	Tohoku region	The Sea of Japan side of eastern Japan	The Pacific side of eastern Japan	The Sea of Japan side of western Japan	The Pacific side of western Japan
Rank 1	2020 (55%)	2020 (40%)	2020 (41%)	2020 (50%)	2020 (57%)
Rank 2	2006 (55%)	2003 (50%)	2003 (50%)	2009 (52%)	1993 (58%)
Rank 3	2003 (55%)	2009 (51%)	1993 (55%)	2003 (52%)	1954 (64%)

Statistics began in 1946

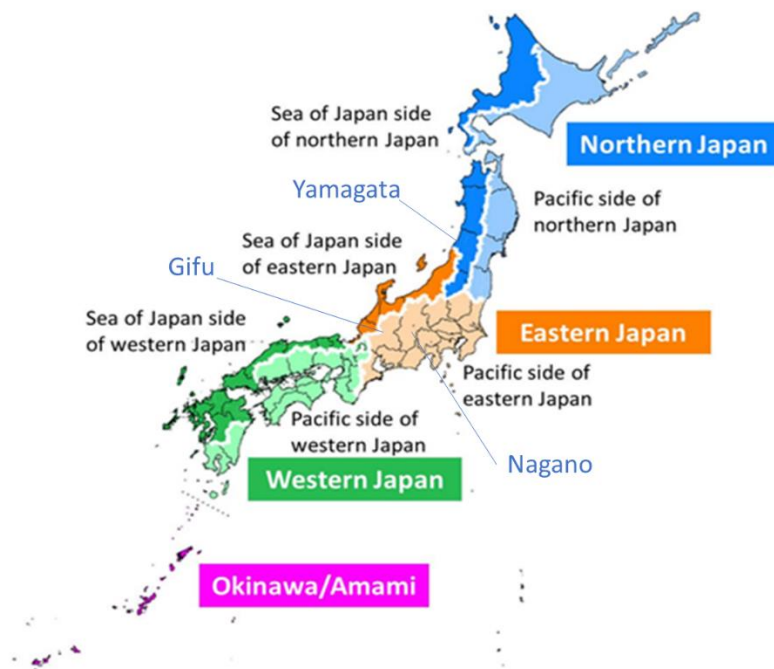


Figure A1. Climatological regions of Japan

The JMA defines seven regional divisions for climate monitoring and forecast (the Sea of Japan sides and the Pacific sides of northern, eastern, western Japan, and Okinawa/Amami).